Renewable Energy 184 (2022) 975–989

Contents lists available at ScienceDirect

Renewable Energy

journal homepage: www.elsevier.com/locate/renene

Simultaneous short-term significant wave height and energy flux prediction using zonal multi-task evolutionary artificial neural networks

A.M. Gómez-Orellana [1], D. Guijo-Rubio [*,1], P.A. Gutiérrez , C. Hervás-Martínez

Department of Computer Science and Numerical Analysis, University of Córdoba, Córdoba, Spain

ARTICLE INFO

Article history:
Received 6 May 2021
Received in revised form
20 November 2021
Accepted 30 November 2021
Available online 9 December 2021

Keywords:
Wave height prediction
Energy flux prediction
Marine energy
Multi-task machine learning
Zonal models
Evolutionary artificial neural networks

ABSTRACT

The prediction of wave height and flux of energy is essential for most ocean engineering applications. To simultaneously predict both wave parameters, this paper presents a novel approach using short-term time prediction horizons (6h and 12h). Specifically, the methodology proposed presents a twofold simultaneity: 1) both parameters are predicted by a single model, applying the multi-task learning paradigm, and 2) the prediction tasks are tackled for several neighbouring ocean buoys with such single model by the development of a zonal strategy. Multi-Task Evolutionary Artificial Neural Network (MTEANN) models are applied to two different zones located in the United States, considering measurements collected by three buoys in each zone. Zonal MTEANN models have been compared in a two-phased procedure: 1) against the three individual MTEANN models specifically trained for each buoy of the zone, and 2) against some state-of-the-art regression techniques. Results achieved show that the proposed zonal methodology obtains not only better performance than the individual MTEANN models, but it also requires a lower number of connections. Besides, the zonal MTEANN methodology outperforms state-of-the-art regression techniques. Hence, the proposed approach results in an excellent method for predicting both significant wave height and flux of energy at short-term prediction time horizons.

1. Introduction

The wide range of operations being performed in offshore locations has widely increased the interest in the accurate prediction of wave features [1,2]. Specifically, activities such as maritime traffic [3], fishing [4,5], design, planning and maintenance of offshore structures [6–8] or development and management of renewable sources of energy [9,10], to name a few, depend on wave parameters such as the significant wave height or the flux of energy, which may be the most important variables in this regard. Thus, the study carried out in this paper is focused on these two parameters. For this purpose, the framework of the linear wave theory is considered to define the parameters involved in setting a given sea state and its derived wave energy estimation [11]. On the one hand, the significant wave height not only does it have great impact on previously listed human and economic activities, but it also plays an essential role in some climate processes [12,13] and in the forecasting of cyclones, earthquakes and tsunamis that may occur in the ocean [14]. Significant wave height is directly measured by sensors integrated in the ocean buoys, providing real-time reliable information of the sea state [15,16]. On the other hand, focusing on the impact that fossil fuels (such as oil, natural gas or coal) have on climate change, there is a huge necessity of turning these non-renewable sources of energy into green ones, by developing new methodologies able to efficiently exploit the natural resources available in our environment. In this sense, marine energy has turned out, in the last years, to be one of the most promising sources of clean energy [17,18]. The reason behind this fact is twofold: 1) unlike solar energy, which is only generated during daylight hours, tidal and wave energies do through the whole day, and 2) there are numerous coastal areas that can benefit from these types of energy [19,20]. Accurately estimating the energy flux is important for the production of energy, which is performed by converting kinetic energy from waves into electricity using wave

* Corresponding author. Department of Computer Science and Numerical Analysis, University of Cordoba, Rabanales Campus, Albert Einstein Building, 3rd Floor, 14 014, Córdoba, Spain.
E-mail address: dguijo@uco.es (D. Guijo-Rubio).
[1] A. M. Gómez-Orellana and D. Guijo-Rubio contributed equally to this work.

https://doi.org/10.1016/j.renene.2021.11.122

energy converters [11,21,22].

The prediction of both wave parameters (significant wave height and flux of energy) has been widely studied in the literature. Although approaches considering physical models [23,24] or statistical techniques [25–27] still come up to address wave characterisation, the interest in them has decreased in the last few years in favour of Machine Learning (ML) methods [28], which has proved to be accurate when applied to this field [11,29].

In this way, one of the first works dealing with the prediction of significant wave height by using a ML technique was proposed in Ref. [30], where Artificial Neural Networks (ANNs) were applied, trained by means of a back-propagation algorithm for real-time significant wave height forecasting along the east coast of India. Note that ANNs have been widely applied in the literature over the years. In Ref. [31], a two-phased ANN was employed for the prediction of significant wave height and zero-up-crossing wave period at four different warning times (3h, 6h, 12h and 24h). More recently, in Ref. [32], ANNs were applied to a nearshore wave power prediction problem over two buoys located in the northern coast of Spain, in which 12 different architectures containing one or two hidden layers were assessed. In Ref. [33], ANNs optimised by different algorithms (Levenberg-Marquardt, gradient descent, Bayesian regularisation or conjugate gradient) were applied to wind and wave data to predict the significant wave height in the Bay of Bengal, northern Indian ocean, the combination of ANN with Bayesian regularisation being the most effective algorithm [34]. proposed the use of Recurrent Neural Networks (RNNs) for the wave prediction at four time horizons (3h, 6h, 12h and 24h) in the Caspian Sea, in the north of Iran, obtaining excellent results in terms of correlation coefficient. Moreover, apart from ANNs, there are other ML techniques applied to this problem, as in Ref. [35], in which significant wave prediction for two buoys located in the Adriatic Sea was carried out not only by ANNs but also by Support Vector Machines (SVMs). In Ref. [36], the well-known Extreme Learning Machine (ELM) algorithm was used for developing an ensemble able to predict the daily significant wave height in ten buoys located in the Gulf of Mexico, Brazil and Korean region. Regarding deep learning techniques, in Ref. [37], Convolutional Neural Networks (CNNs) were applied for real-time wave height estimation from solely raw ocean images in a two-phased approach: first, four structures of CNNs are trained, and then the accuracy achieved by these four CNNs is improved by the application of a Long Short-Term Memory (LSTM) based regression model to a sequence of ocean images. Besides, in Ref. [38] a hybrid model denominated STL-CNN-PE was proposed for significant wave height forecasting using meteorology data from ocean buoys. LSTMs have also been applied by Ref. [39] in order to predict the significant wave height at 1h and 6h time horizons over ten stations (located in Korea, Brazil, Spain, UK and USA) with different environmental conditions. Regarding flux of energy prediction, there are also numerous works presented in the literature in the last years [40]: proposed an ANN-based model to assess the wave energy potential in Brazil. Furthermore [41], proposed the use of deep learning ANNs trained following moth-flame optimisation for parameter selection. This methodology was tested over 13 buoys from different locations (Pacific and Atlantic Coasts and the Gulf of Mexico) [42]. applied multi-task ANNs for the prediction of the flux of energy in the Gulf of Alaska at several time prediction horizons, combining short- and long-term time horizons (6h, 12h, 24h and 48h).

Moreover, both prediction tasks (significant wave height and flux of energy prediction) have been combined in some previous works [43]. proposed a novel hybrid approach combining grouping genetic algorithms with ELMs for the prediction of both tasks at the Western Coast of the USA. In Ref. [44], the application of a genetic fuzzy system for regression was used for estimating both parameters from neighbouring buoys [2]. presented the Bayesian optimisation of a hybrid grouping genetic algorithm for attribute selection combined with ELM for the prediction of significant wave height and energy flux. On the other hand [29], also tackled the prediction of these two parameters, but focusing on ordinal classification, i.e. both prediction tasks were considered as ordinal multi-class classification problems by dicretising the real variables in several categories, simplifying, in this way, the original problem. These categories showed an order, which was taken into account by the ordinal classifiers.

Therefore, following the idea of these last works, the simultaneous prediction of both parameters has a huge and valuable interest for many diverse aforementioned applications. Besides, the relationship between two different tasks can be exploited by means of Multi-Task Learning (MTL) [45]. MTL is a ML paradigm taking advantage from the relationships existing between related tasks [46,47], such is the case of significant wave height and energy flux prediction. Thus, models following MTL can infer such latent information, improving its performance with respect to individual models for each task. On the other hand, the short-term prediction is of relevant interest given that it provides a balance between anticipation and accuracy, i.e. when the prediction is performed at a long-term time horizon, having time to anticipate to certain events, it is highly likely that the accuracy of the models decreases, given that numerous events could occur in between. On the contrary, estimation, which consists on determining the output variables from input attributes at the same time instant, does not allow the anticipation to any event but the results will be more accurate. Hence, short-term prediction, i.e. 6h and 12h time prediction horizons, establishes an appropriate balance between anticipation and accuracy, which is interesting for the tasks considered in this paper.

Despite the numerous works presented in the literature carrying out the prediction of significant wave height or energy flux, none of them, up to the knowledge of the authors, considers the application of a grouping methodology for developing a single model able to predict the wave parameters over several neighbouring buoys located in the same zone. With this “grouping” term, we refer to share information between neighbouring buoys, which are by definition located in the same zone. In this sense, the models are built using a wider range of characteristics (the events of all the buoys in the zone), providing these models with more particular casuistry. Besides, the interest in these models is reinforced due to the fact that they could be used to predict within the area delimited by the buoys of the zone. Even though these models could be thought to be more complex and time consuming, they are quite the opposite, given that only one model performs the prediction of both parameters for all the buoys, being, in this way, simpler than the combination of single models trained in each buoy located in the zone.

In this paper, we propose the application of Multi-Task Evolutionary Artificial Neural Networks (MTEANNs), which have been proved to be excellent when applied to problems related to the estimation of ocean wave parameters. Specifically, we focus on significant wave height and energy flux, the two most important parameters in this regard. Moreover, given that changes in the ocean behaviour are highly unforeseen, accurate prediction of both wave parameters is of enormous interest in ocean engineering activities. Consequently, such prediction is carried out at a short-term, 6h and 12h time prediction horizons. In addition, due to the fact that similar behaviours are likely to be experienced by nearby buoys though at different time, a zonal strategy is proposed,

i.e. one single model is trained able to accurately predict both parameters on several buoys simultaneously. This helps improve the characterisation of waves and, therefore, increase the performance achieved by local models individually designed for each buoy. We consider two different coastal zones: the Gulf of Alaska (Alaska) and the South West Coast of USA (California), each of them with three buoys. Results achieved by the MTEANNs using the proposed zonal strategy are compared in a two-phased procedure: 1) against MTEANNs individually trained for each buoy, and 2) against some popular state-of-the-art regression techniques benefiting also from using the zonal strategy, providing, in this sense, a comprehensive comparison.

The remaining of this article is structured as follows: Section 2 details the two sources of information considered and the preprocessing and integration steps performed for obtaining the dataset used. Section 3 describes the proposed zonal methodology for predicting the significant wave height and the flux of energy, as well as the local strategy for comparison purposes, using a MTL methodology applied to the EANNs models. Section 4 shows the experimental settings and the results obtained, including an analysis of the performance of the different techniques evaluated. Finally, Section 5 outlines some conclusions and future work.

2. Data description and processing

In this section, the data used in this research and the preprocessing performed are specified. The data has been obtained from two different sources of information: from the *National Data Buoy Center* (NDBC) [48] and from the *National Center for Atmospheric Research* (NCAR) [49,50]. On the one hand, NDBC provides meteorological and oceanographic observations for the marine environment, collected by buoys deployed along the United States of America (USA) coastal regions. Data is recorded in real-time by sensors installed in the buoys and includes measurements such as significant wave height, dominant wave period and average wave period, among others. On the other hand, NCAR provides climatological data on a 2.5° latitude-longitude grid. Data collected from diverse sources (e.g. ships, rawinsondes, satellites, etc.) is first quality controlled and assimilated, and then, a climate model obtains reanalysis-gridded variables including surface pressure, zonal wind and meridional wind, among others.

For this study, we have considered the measurements of six buoys located in two important coastal zones, the Gulf of Alaska and the South West Coast, both located in the USA, hourly recorded from year 2015–2018. Furthermore, regarding the reanalysis data, we have selected seven climatological variables for the same time period, with four values every day.

A combination of both kind of data has been considered as input variables for characterising ocean events: all the reanalysis variables along with the information obtained from past values of the two observed measurements. On the other hand, for obtaining the output variables, measurements recorded by the buoys under study have been studied. A detailed description of this data is provided in the following subsections.

2.1. Buoys measurements

As mentioned above, we have considered two relevant zones from the USA: the Gulf of Alaska and the South West Coast. For each of these two zones, three buoys have been selected. In Fig. 1 the location of each of these six buoys is represented. They have been chosen considering their geographical location in each zone (distance and depth of water) with the aim of providing a better characterisation of the zone under study:

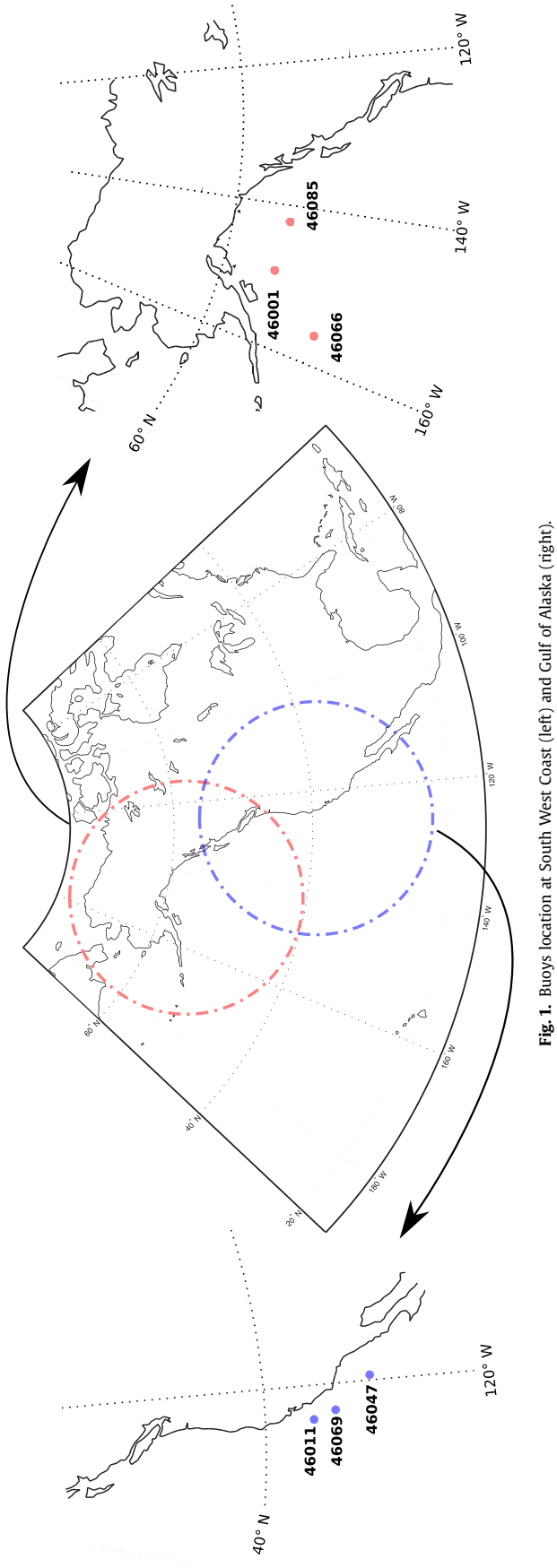

Fig. 1. Buoys location at South West Coast (left) and Gulf of Alaska (right).

- South West Coast:
  - Buoy 46 011 (LLNR 215) [51] - Santa Maria - 21NM NW of Point Arguello, CA. Geographical location: 34.956N 121.019W
  - Buoy 46 047 (LLNR 82) [52] - Tanner Bank - 121NM West of San Diego, CA. Geographical location: 32.404N 119.506W
  - Buoy 46 069 (LLNR 181.6) [53] - Santa Rosa - South Santa Rosa Island, CA. Geographical location: 33.677N 120.213W
- Gulf of Alaska:
  - Buoy 46 001 (LLNR 984) [54] - Western Gulf of Alaska - 175NM SE of Kodiak, AK. Geographical location: 56.232N 147.949W
  - Buoy 46 066 (LLNR 984.1) [55] - South Kodiak - 310NM SSW of Kodiak, AK. Geographical location: 52.765N 155.009W
  - Buoy 46 085 (LLNR 984.15) [56] - Central Gulf of Alaska - 265NM West of Cape Ommaney, AK. Geographical location: 55.883N 142.482W

As aforementioned, this work focuses on significant wave height (H_s) and energy flux (F_e) prediction. However, the F_e needs to be computed given that it is not real-time recorded by the buoys. To do that, and considering the linear wave theory, two wave parameters recorded by the buoys, the H_s and the average wave period (T_e), are used as follows:

$$F_e = 0.49 \cdot H_s^2 \cdot T_e, \quad (1)$$

where F_e is expressed in kW/m (kilowatts per metre), H_s is expressed in m (metres) and T_e is expressed in s (seconds). Given that H_s represents a sort of average wave height, F_e is computed in Eq. (1) as an average flow of energy, even though, to simplify it will be simply denoted as energy flux.

In this way, when obtaining the datasets, the three buoys measurements considered will be the average wave period, the significant wave height, and the energy flux.

2.2. Reanalysis data grid

Waves and, as a result, energy flux, are mainly originated by the action of the wind. However, other important elements play a key role in a better modelling of the environment. In this sense, the reanalysis variables have been selected aiming to provide a good representation of the wind behaviour as well as an useful description of other weather conditions [42]. In Table 1, the reanalysis variables considered are shown.

As mentioned above, NCAR provides reanalysis data gridded on a 2.5° latitude-longitude grid, representing each grid a reanalysis node. In this way, to model the weather conditions related to each buoy, a sub-grid composed of four reanalysis nodes is considered. More specifically, the four closest reanalysis nodes to the geographical location of each buoy are used. For the sake of clarity, Fig. 2 approximately represents the sub-grid corresponding to Buoy 46 069 (West South Coast). In this way, six sub-grids of reanalysis data is selected, one for each buoy under study, which are detailed in Table 2.

Table 1
Reanalysis variables considered.

Variable	Description	Units
air	Air temperature	K
vwnd	Component South-North of wind speed	m/s
uwnd	Component West-East of wind speed	m/s
omega	Omega vertical velocity	Pa/s
pr_wtr	Precipitable water content	kg/m^2
pres	Pressure	Pa
rhum	Relative humidity	%

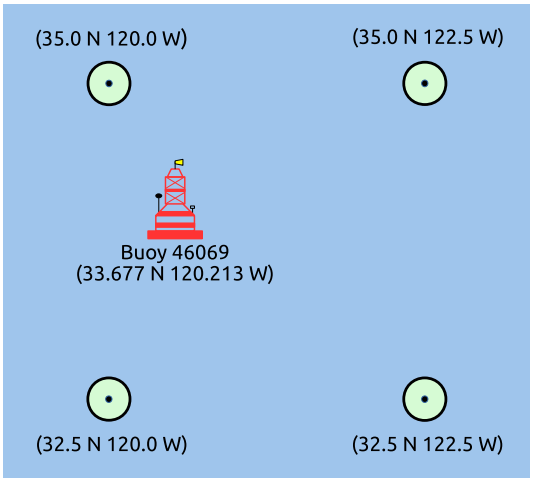

Fig. 2. Sub-grid representation of the four closest nodes of reanalysis that surround the Buoy 46 069 from the South West Coast.

2.3. Obtaining the datasets

Given that two sources of information are considered (NDBC and NCAR), it is necessary to perform a data integration process to combine such information and obtain the datasets. Prior to such process, missing values of buoys measurements are recovered due to the fact that measurements are real-time collected and they may be incomplete as a consequence of weather conditions or sensor failures. Specifically, the procedure of missing values recovery was only performed for the significant wave height and average wave period measurements (necessary for the energy flux computation). Therefore, it is worthy of mentioning that the number of total missing values recovered was negligible. Reanalysis data is obtained by a climate model, i.e. data is always available and it is not necessary to deal with missing values.

The objective of the data integration is to combine buoys measurements (hourly collected from 00 : 50h to 23 : 50h) and reanalysis variables (4-times daily: 00h, 06h, 12h and 18h). For this purpose, we used the SPAMDA software tool [57], which is specifically designed to perform this task and greatly simplify it through a *matching* procedure. The values of the parameters used to perform the *matching*[2] procedure are the following:

- Output: flux of energy (F_e).
- Reanalysis variables: air, omega, pr_wtr, pres, rhum, uwnd and vwnd (see Table 1).
- Buoy attributes: significant wave height (H_s) and average wave period (T_e).
- Number of nearest reanalysis nodes to consider: 4.
- Number of final datasets: 1 (using the weighted mean of the 4 reanalysis nodes considered).
- Prediction task: regression.

In this way, one dataset for each of the buoys is obtained. More specifically, each dataset consists of nine input variables (the seven

[2] Further details of the *matching* process along with the parameters considered can be found in Ref. [57].

Table 2
Sub-grid of reanalysis nodes for each buoy.

Zone	Buoy ID	Geographical locations	Nodes of reanalysis (latitude N, longitude W)			
		(latitude N, longitude W)	Node 1	Node 2	Node 3	Node 4
South West Coast	46 011	(32.5N–35.0N, 120.0W–122.5W)	(32.5N, 122.5W)	(32.5N, 120.0W)	(35.0N, 122.5W)	(35.0N, 120.0W)
	46 047	(30.0N–32.5N, 117.5W–120.0W)	(30.0N, 120.0W)	(30.0N, 117.5W)	(32.5N, 120.0W)	(32.5N, 117.5W)
	46 069	(32.5N–35.0N, 120.0W–122.5W)	(32.5N, 122.5W)	(32.5N, 120.0W)	(35.0N, 122.5W)	(35.0N, 120.0W)
Gulf of Alaska	46 001	(55.0N–57.5N, 147.5W–150.0W)	(55.0N, 150.0W)	(55.0N, 147.5W)	(57.5N, 150.0W)	(57.5N, 147.5W)
	46 066	(52.5N–55.0N, 155.0W–157.5W)	(52.5N, 157.5W)	(52.5N, 155.0W)	(55.0N, 157.5W)	(55.0N, 155.0W)
	46 085	(55.0N–57.5N, 140.0W–142.5W)	(55.0N, 142.5W)	(55.0N, 140.0W)	(57.5N, 142.5W)	(57.5N, 140.0W)

weighted reanalysis variables and the two buoys attributes) and four output variables (H_s and F_e at 6h and 12h). Since the prediction horizons are tackled at t + 6h and t + 12h time instants, as a novelty, autoregressive (AR) models have been considered. The reason behind using these models is that many observed time series show serial autocorrelation, and such is the case of H_s and F_e. Exploiting this correlation by including past values of the target variables could lead to more accurate estimations. In this sense, to build the AR model, the variables H_s and T_e at the previous instant (t) are used as inputs.

As a result of the matching process, the dataset of each buoy contains 5844 instances comprising the time period from 2015 to 2018. In Table 3, statistical features associated to the significant wave height and the flux of energy are shown. As can be checked, the two zones present diverse characteristics.

3. Methodology

This section describes the Multi-Task Evolutionary Artificial Neural Network (MTEANN) models considered in this work, as well as the Evolutionary Algorithm (EA) used for tuning the ANN structure and weights. In addition, the proposed zonal methodology is also introduced.

3.1. Multi-task Artificial Neural Networks

Artificial Neural Networks (ANNs) [58] have become a relevant support in an enormous diversity of research studies owing to the abilities and properties they have. Indeed, they are frequently applied to solve many real-world problems related to regression and classification tasks, yielding excellent performance. Multilayer Perceptron (MLP) [58] is the most widely used neural network architecture. A MLP consists of one input layer, one or more hidden layers and one output layer.

As aforementioned, this work focuses on significant wave height and energy flux short-term prediction (6h and 12h). Given that both wave parameters are simultaneously predicted, the multi-task regression paradigm is considered to address the problem under study, which is formulated as follows:

$$D = \{(\mathbf{x}_i, y_{H_{i6h}}, y_{F_{i6h}}, y_{H_{i12h}}, y_{F_{i12h}}); i = 1, 2, \ldots N\}, \quad (2)$$

where D represents the input data used, $\mathbf{x}_i$ is the vector containing the seven weighted reanalysis variables and the two buoys attributes, $y_{H_{i6h}}$, $y_{H_{i12h}}$, $y_{F_{i6h}}$ and $y_{F_{i12h}}$ are the significant wave height and the energy flux at both time prediction horizons, and N represents the number of instances.

Therefore, a multi-task ANN regression model is considered to tackle the problem described. Specifically, the model has nine input neurons (one for each input variable) and four outputs, which simultaneously predict both wave parameters at both time prediction horizons. In this way, and regardless the hidden layer, the estimated function $f_q(\mathbf{x}, \mathbf{w}, \beta)$ from each output is given as follows:

$$f_q(\mathbf{x}, \mathbf{w}, \beta) = \beta_{q0} + \sum_{j=1}^{m} \beta_{qj} B_j(\mathbf{x}, \mathbf{w}_j), \quad q = 1, \ldots, Q, \quad (3)$$

where $Q = 4$ is the number of outputs of the problem, $B_j(\mathbf{x}, \mathbf{w}_j)$ is the activation function of each hidden neuron, which applies the nonlinear transformations of the vector $\mathbf{x}^T = (x_1, x_2, \ldots, x_d)$ with d input variables (d = 9, in this study); $\beta_q^T = (\beta_{q0}, \beta_{q1}, \beta_{q2}, \ldots, \beta_{qm})$ represents the coefficients of the synaptic weights from hidden layer to output layer, including the element β_{q0} as bias; $\mathbf{w}_j^T = (w_{j0}, w_{j1}, \ldots, w_{jd})$ stands for the weights of the connections from input layer to each of the m activation functions of hidden layer, w_{j0} representing the bias.

Regarding the neurons in hidden layer, Sigmoidal Units (SUs) [59] have been selected. SU is probably the most widely used activation function, and it has achieved excellent performance when tackling regression problems [42]. According to the notation used, SU activation function is given by the following expression:

$$B_j(\mathbf{x}, \mathbf{w}_j) = \frac{1}{1 + e^{-\left(w_{j0} + \sum_{i=1}^{d} w_{ji} x_i\right)}}, \quad j = 1, \ldots, m, \quad (4)$$

where w_{j0} is the bias. Fig. 3 illustrates the architecture of the ANNs considered.

Table 3
Statistical features associated to the significant wave height and the flux of energy for all the buoys. SD stands for Standard Deviation.

Zone	Buoy ID	Statistical features							
		Significant wave height (H_s, m)				Flux of energy (F_e, kW/m)			
		Min	Max	Mean	SD	Min	Max	Mean	SD
South West Coast	46 011	0.66	8.02	2.04	0.86	1.01	412.24	19.37	23.61
	46 047	0.71	6.67	2.08	0.85	1.33	275.98	19.39	21.84
	46 069	0.64	7.68	2.08	0.81	0.80	387.86	18.82	21.17
Gulf of Alaska	46 001	0.36	9.90	2.62	1.36	0.29	518.67	31.11	41.26
	46 066	0.60	12.07	2.86	1.52	0.82	938.72	41.44	61.59
	46 085	0.41	8.71	2.65	1.37	0.26	350.65	31.76	40.30

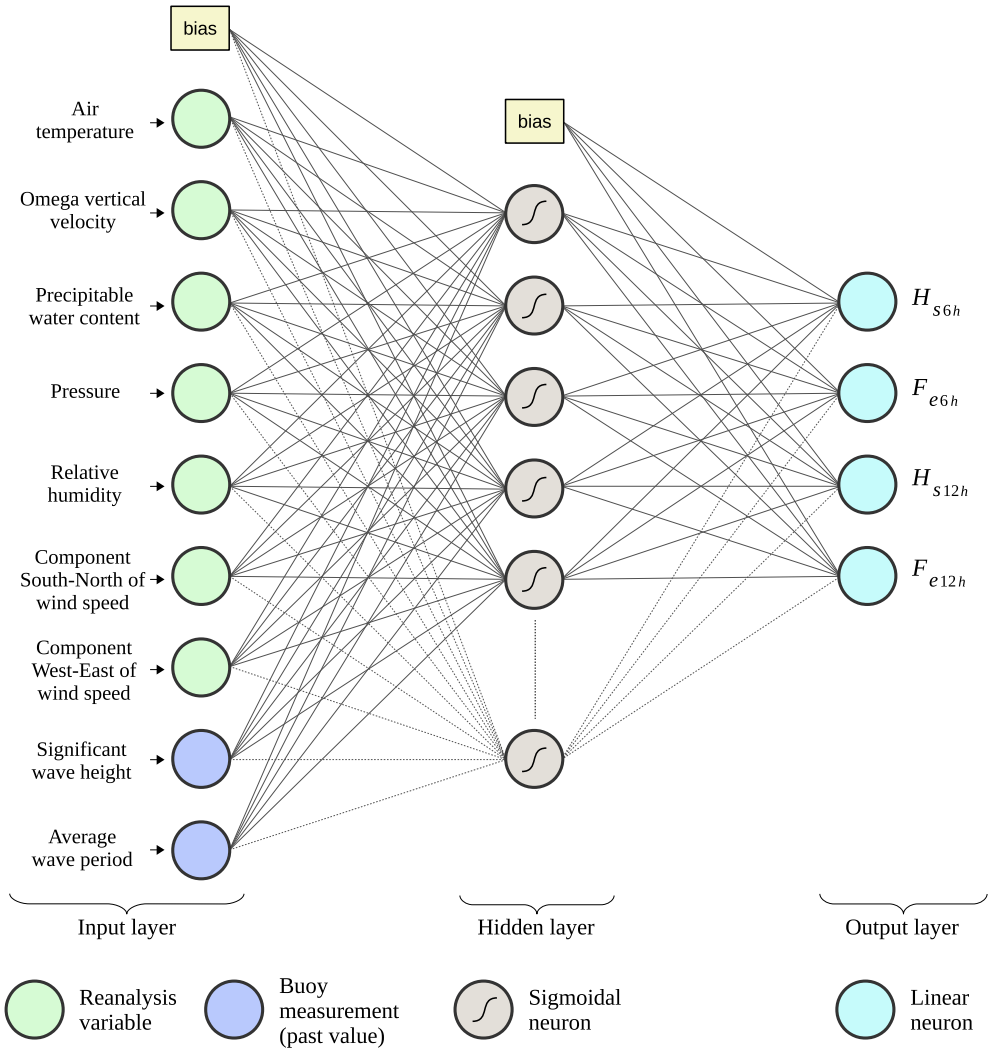

Fig. 3. ANN architecture.

3.2. Evolutionary Algorithms

Gradient-based methodologies, such as back-propagation algorithm, have been widely used to train ANNs. Nevertheless, these methods can be trapped in local optima due to the convoluted error surface associated with neural network models. In this sense, EAs not only were proposed as a valuable approach for fitting the weights and structure of ANNs but also have achieved excellent results [60], without considering the initial search conditions.

Therefore, in this work, an EA is used for optimising the architecture of the ANNs considered. This algorithm is described in Algorithm 1, resulting in MTEANNs.

Algorithm 1. Evolutionary Algorithm

randomly generate an initial population of size Np of ANNs, considering the structure defined in Eq. 3.
repeat
  calculate the MSE of each ANN
  rank the ANNs with respect to their MSE
  clone the best 10% of the ANNs, which replaces the worst 10%
  apply parametric mutation to the best 10% of the ANNs
  apply structural mutation to the remaining 90% of the ANNs
until *stopping criteria is fulfilled*
return *the ANN with lowest MSE as final solution*

As can be seen, the algorithm starts by generating a random initial population of ANNs. Next, the population is evaluated and ranked with respect to its Mean Squared Error (MSE, see Eq. (5)), and then the best 10% of the ANNs is cloned, which replaces the worst 10%. After that, parametric and structural mutations are carried out to evolve the population. Such evolutionary process is repeated until the stopping criteria is fulfilled. Finally, the ANN with lowest MSE is returned as the solution to the problem.

Specifically, parametric mutation updates the coefficients of the synaptic weights of each ANN, using an additive Gaussian noise which has a normal distribution with 0 mean, and whose variance decreases during the evolution.

On the contrary, structural mutation alters the structure of each ANN to explore different topologies in terms of number of neurons and number of synaptic weights. Such exploration is carried out by applying the following types of structural mutations: delete neuron, add neuron, neuron fusion, delete link and add link. The EA does not consider the crossover operator because it has been shown to be inefficient when evolving ANNs [61].

Throughout the evolution, the performance of each individual of the population is optimised with respect to the MSE, which is expressed as an average of MSE of each of the $Q = 4$ outputs, defined as follows:

$$MSE(\mathbf{x}, \mathbf{w}, \boldsymbol{\beta}) = \frac{1}{Q}\sum_{q=1}^{Q} MSE_q(\mathbf{x}, \mathbf{w}, \boldsymbol{\beta}) = \frac{1}{Q}\sum_{q=1}^{Q}\left(\frac{1}{N}\sum_{i=1}^{N}\left(y_i^q - f_q(\mathbf{x}, \mathbf{w}, \boldsymbol{\beta})\right)^2\right), \quad (5)$$

where $MSE_q(\mathbf{x}, \mathbf{w}, \beta)$ is the MSE for the q-th output, $f_q(\mathbf{x}, \mathbf{w}, \beta)$ is the ANN output defined in Eq. (3), N represents the number of instances, and y_i^1, y_i^2, y_i^3 and y_i^4 correspond to $y_{H_{i6h}}$, $y_{F_{i6h}}$, $y_{H_{i12h}}$ and $y_{F_{i12h}}$, respectively, i.e. the significant wave height and the energy flux at both time prediction horizons for instance i, as described in Eq. (2).

In this way, MTEANNs using SUs as activation functions (for the neurons in hidden layer) and four linear outputs will be studied. The Standard Error of Prediction (SEP) will also be used for comparing the performance of MTEANNs, which is defined as follows:

$$SEP(\mathbf{x}, \mathbf{w}, \boldsymbol{\beta}) = \frac{1}{Q}\sum_{q=1}^{Q}\frac{100}{\bar{y}_q}\sqrt{MSE_q(\mathbf{x}, \mathbf{w}, \boldsymbol{\beta})} = \frac{1}{Q}\left(\sum_{q=1}^{Q}\frac{100}{\bar{y}_q}\sqrt{\frac{1}{N}\sum_{i=1}^{N}\left(y_i^q - f_q(\mathbf{x}, \mathbf{w}, \boldsymbol{\beta})\right)^2}\right), \quad (6)$$

where $\bar{y}_q$ is the average value of the q-th output for all instances in dataset. The SEP expresses a relative error (represented as a percentage) and has the advantage of being dimensionless.

3.3. Zonal methodology

In order to improve the characterisation of waves, we propose a zonal methodology that groups and shares the information provided by the buoys located in the same zone. Specifically, the zonal methodology groups the instances of all buoys in the zone under study, that is, the information is combined by concatenating vertically the datasets. In this way, with this grouping the characterisation of the problem being tackled is enhanced due to the fact that the training phase considers the information provided by all

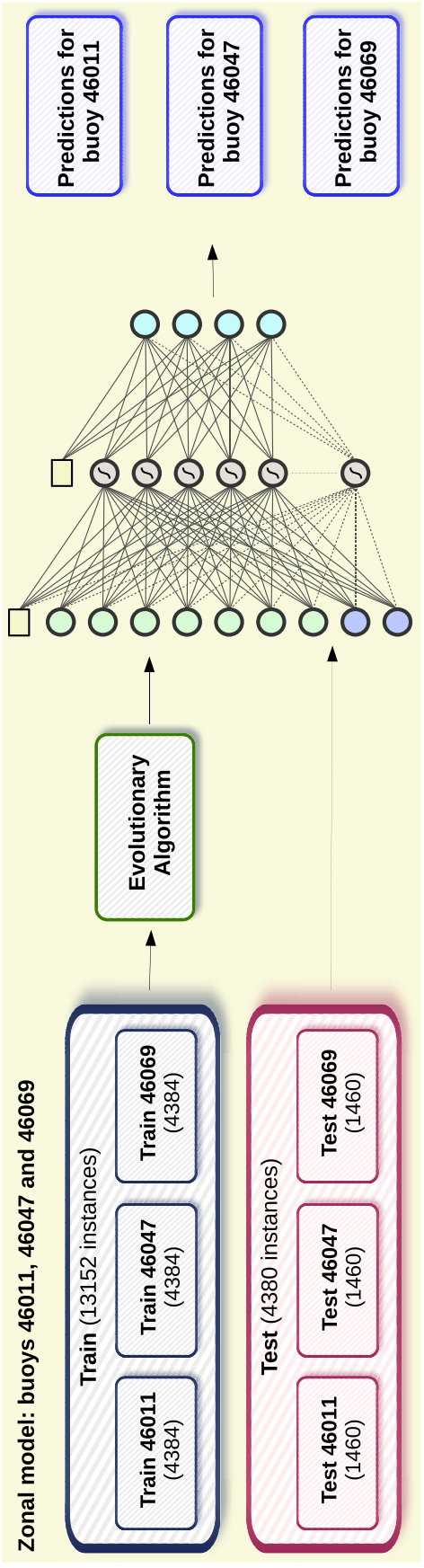

Fig. 4. Example of the zonal methodology corresponding to the South West Coast zone.

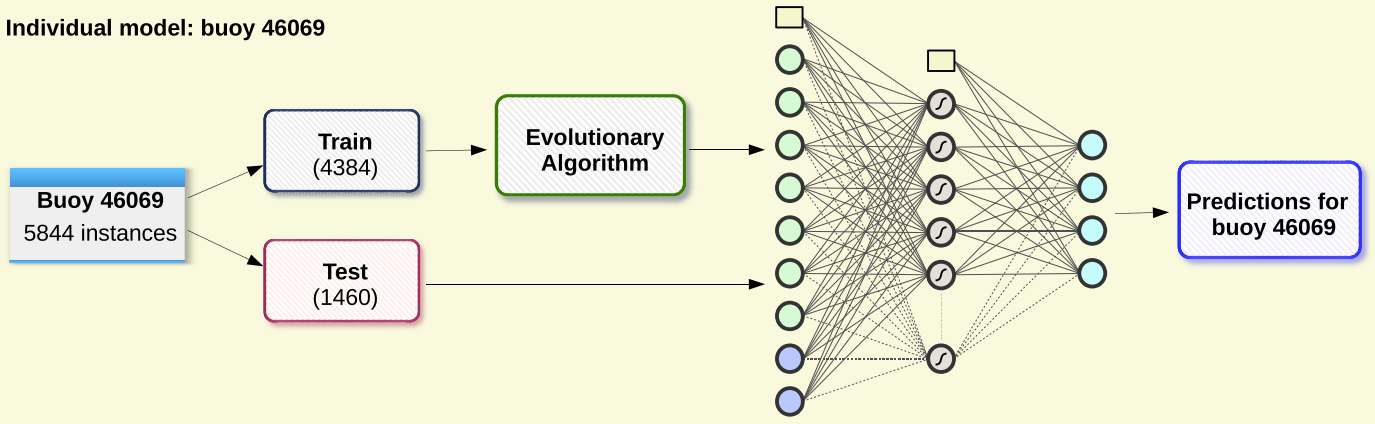

Fig. 5. Example of the local methodology corresponding to the buoy 46 069 of the South West Coast zone.

the buoys in the zone. Being of great utility to better understand and model the atmospheric processes of the zone, that could lead to better prediction models.

In Fig. 4, the proposed methodology applied to the South West Coast zone is illustrated. As can be seen, the training set used by the EA is composed of the training sets belonging to the buoys 46 011, 46 047 and 46 069, that is, it is formed by the instances of the three buoys. In this way, the trained model can take advantage of similar behaviours experienced by the buoys in the zone, but temporally different due to the distance between them. Hence, the performance of the model can be improved using this strategy.

In addition, the model can infer a wider range of characteristics and patterns using this zonal methodology, benefiting from a rich and varied description of the environmental factors existing in the zone. Therefore, using the proposed methodology, a single model can be developed to perform both prediction tasks over all the buoys located in the same zone, as shown in Fig. 4. Thus, this methodology is less complex given that only one model is developed instead of one for each buoy in the zone. Furthermore, given that the grouping is vertically carried out (considering instances instead of variables), the input variables are the same and the complexity of the zonal model is not increased.

In order to assess the feasibility of the proposed zonal methodology, and for comparison purposes, a local methodology that considers individually trained models is used. In Fig. 5, the individual model corresponding to the buoy 46 069 of the South West Coast zone is represented. In this case, the EA only uses the training set belonging to the buoy being studied, without considering the remaining ones. Hence, one model for each of the buoys in the zone under study will be developed.

4. Experimental settings and results

In this section, the experimental settings used for the MTEANN model are described, as well as those for the main state-of-the-art approaches in regression. Besides, the results obtained for the comparison between all these models are also presented.

4.1. Experimental settings

As previously specified in Section 3, in this paper we propose a zonal strategy for tackling the significant wave height and the flux of energy predictions. In this sense, the original datasets (described in Section 2) are divided into two different sets, following the guidelines specified in Ref. [62]: the first 75% of the data is used for training the models (i.e. the first three years, 2015–2017), whereas the remaining 25% is used for testing the performance of the models (year 2018). Hence, in the case of the proposed zonal strategy (one dataset per zone, in this paper, two datasets), the training and the test sets of each zone are composed of 13, 152 and 4, 380 instances, respectively. Moreover, in order to demonstrate the ability of the zonal strategy in comparison against the local methodology, the datasets used for this local approach have also been built following the previous guidelines. Thus, when the local strategy is considered (one dataset per buoy, a total of six datasets), the training and the test sets of each buoy are composed of 4, 384 and 1, 460 instances, respectively.

All the MTEANN models, regardless of the strategy used, have been trained using the following parameters: the algorithm has been run 40 times with 600 of population size and using 5, 000 generations. As aforementioned in Section 3.1, in this paper, SUs have been chosen for the hidden layer, initialising the number of hidden nodes in the range [1,10], whereas the output layer is composed of four linear units. Regarding the number of nodes and links to be created or deleted, they are randomly selected in the ranges [1,5,7], respectively. Furthermore, the range [− 10, 10] is used for initialising all the weights between the three layers (input to hidden layer and hidden to output layer). In addition, the nine input variables have been scaled to the range [0.1, 0.9] before the application of the MTEANN models[3].

Moreover, an extensive comparison against some state-of-the-art approaches commonly used in the literature for significant wave height and energy flux prediction is also carried out. These techniques are Support Vector Regressor (SVR) [66], Linear Regression (LinearReg) [28], Ridge Regression (RidgeReg) [28], Lasso Regression (LassoReg) [67], and ElasticNet [68]. SVR, LinearReg and RidgeReg are standard regression techniques but can be straightforwardly applied to multi-output problems. On the other hand, LassoReg and ElasticNet can indeed be adapted to multi-task learning. Multi-output regressors do not take into account the relation between the outputs, i.e. different models are built for each output, whereas, multi-task regressors infer a common representation from the related tasks, i.e. a single model is used for predicting both the significant wave height and the energy flux simultaneously. In addition, these five techniques have a deterministic nature, and, therefore, they have been run once.

[3] Further information of the parameters considered can be found in Refs. [63–65], whereas, more information regarding the ANN models can be obtained from Ref. [58].

For tuning the parameters of these regression techniques, a 10-fold cross-validation over the training set is used, and the best parameters are selected according to the lowest MSE. More specifically, the SVR kernel width is tuned using the range $\{10^{-3}, 10^{-2}, \ldots, 10^{3}\}$. The regularisation parameter of the RidgeReg, LassoReg and ElasticNet techniques is adjusted in the range $\{10^{-3}, 10^{-2}, \ldots, 10^{3}\}$ and the ratio of the L1 penalisation weight for the ElasticNet is tuned using the range [0.10, 0.50, 0.70, 0.90, 0.95, 0.99, 1.00].

Furthermore, with the aim of improving the readability of this paper, the models trained by following the zonal strategy will be named accordingly using the subscript $_Z$, otherwise, when trained by following the local strategy, the subscript $_L$ will be used, e.g. the MTEANN$_Z$ model is a MTEANN model trained by the zonal strategy, whereas MTEANN$_L$ uses the local methodology.

Concerning the computational resources, all the experiments have been run on the same multiprocessor computer, using an Intel© Xeon© Gold 6138 CPU @ 2.00 GHz processor with 192GiB of memory. The code used in this work has been developed by the authors using Java programming language.

4.2. Results

For the sake of clarity, the experiments have been divided in a two-phased procedure: 1) the proposed zonal methodology has been compared against three individual local models (i.e. one per buoy in the zone), in order to demonstrate the usefulness of predicting the significant wave height and energy flux by using information from neighbouring buoys. This first comparison has been carried out using the MTEANN model described in Section 3, given that its use is one of the proposals of this paper. 2) The MTEANN model using the best strategy resulting from the previous is compared against state-of-the-art techniques, which are trained considering the strategy achieving the best results in the previous phase (i.e. zonal or local). This second comparison is carried out in order to demonstrate that the proposed methodology is able to achieve excellent results even when compared against competitive approaches. Moreover, it is worthy of mentioning that both comparisons have been performed in terms of MSE, SEP and number of connections (*#Conn*).

Regarding the first part of the comparison, Table 4 shows the results achieved for both coastal locations (South West Coast and Gulf of Alaska) in terms of MSE and SEP for the four outputs (significant wave height and energy flux considering the 6h and 12h time horizon predictions). Both zonal and local models (i.e. MTEANN$_Z$ and MTEANN$_L$, respectively) have been run 40 times, and the results are expressed as their mean and Standard Deviation (SD): $Mean_{SD}$. In this Table, the proposed MTEANN$_Z$ model is compared against MTEANN$_L$ models for each buoy. For both locations, the MTEANN$_Z$ is the one achieving the best results for all the outputs, with some minor exceptions (2 out of the 24 comparisons for the South West Coast and 4 out of the 24 ones for the Gulf of Alaska, considering both performance measures, MSE and SEP). One of the reasons behind these excellent results is that zonal-trained models use a wider range of patterns enabling the inference of common behaviours, not only geographically, but also temporarily, given that ocean currents can move from one buoy to other neighbouring buoys at a different time. Apart from comparing these models by their performance, it is of relevant interest to compare them by their complexity. In this sense, Table 5 shows the number of connections (*#Conn*) of the zonal model and each local model (*#Conn* Ind.). Note that the local models are trained individually for each buoy, and, therefore, the *#Conn* is the sum of the connections of the three individual models. From this Table, it is obvious that zonal models are much simpler than using individual models, using around three times less connections for both locations.

Therefore, from this first stage of the comparisons, it can be concluded that using zonal models is justified: not only do they outperform the local models (individually-trained for each buoy of the zone) in terms of both performance measures MSE and SEP, but also they are simpler than local models, providing ease of implementation.

On the other hand, the second phase of the comparisons is performed using the zonal strategy, which resulted the best from the previous analysis. This comparison is carried out against the main state-of-the-art regression techniques. Note that these regression approaches also benefit from the zonal methodology, and the aim of this comparison is to prove that MTEANNs are a

Table 4
Comparison between zonal and local MTEANN models (i.e. MTEANN$_Z$ models and MTEANN$_L$ models, respectively) in terms of MSE and SEP for the different buoys located in both coastal zones. The results are expressed as their mean and Standard Deviation (SD): $Mean_{SD}$.

South West Coast									
Buoy	Model	MSE				SEP (%)			
		Significant Wave Height		Energy Flux		Significant Wave Height		Energy Flux	
		6h	12h	6h	12h	6h	12h	6h	12h
46 011	MTEANN$_Z$	**0.098 7$_{0.001\ 4}$**	**0.182 2$_{0.002\ 7}$**	**96.059 4$_{1.701\ 9}$**	**158.027 0$_{4.029\ 3}$**	**15.767 4$_{0.112\ 3}$**	**21.410 8$_{0.156\ 6}$**	**56.255 5$_{0.497\ 6}$**	**72.079 7$_{0.915\ 2}$**
	MTEANN$_L$	0.1 001$_{0.002\ 7}$	0.1 826$_{0.005\ 9}$	97.4 547$_{6.349\ 6}$	158.4 533$_{6.595\ 9}$	15.8 752$_{0.206\ 4}$	21.4 311$_{0.337\ 7}$	56.6 392$_{1.724\ 1}$	72.1 677$_{1.479\ 6}$
46 047	MTEANN$_Z$	**0.093 6$_{0.001\ 6}$**	**0.178 3$_{0.003\ 0}$**	**119.809 6$_{2.720\ 3}$**	200.6 619$_{6.356\ 0}$	**14.892 0$_{0.123\ 3}$**	**20.538 7$_{0.172\ 4}$**	**58.692 9$_{0.663\ 9}$**	75.8 632$_{1.184\ 2}$
	MTEANN$_L$	0.0 961$_{0.005\ 8}$	0.1 786$_{0.004\ 7}$	121.7 024$_{4.378\ 0}$	**199.095 2$_{4.990\ 7}$**	15.0 870$_{0.426\ 9}$	20.5 573$_{0.267\ 8}$	59.1 492$_{1.057\ 3}$	**75.569 8$_{0.941\ 5}$**
46 069	MTEANN$_Z$	**0.098 8$_{0.001\ 8}$**	**0.183 7$_{0.002\ 8}$**	**147.795 6$_{5.074\ 9}$**	**237.545 5$_{4.764\ 3}$**	**15.034 9$_{0.139\ 5}$**	**20.488 0$_{0.155\ 0}$**	**64.092 6$_{1.091\ 8}$**	**81.181 2$_{0.810\ 9}$**
	MTEANN$_L$	0.1 001$_{0.002\ 6}$	0.1 859$_{0.005\ 0}$	153.1 963$_{5.680\ 8}$	243.1 591$_{12.149\ 9}$	15.1 365$_{0.195\ 9}$	20.6 137$_{0.278\ 1}$	65.2 516$_{1.200\ 1}$	82.1 149$_{2.007\ 2}$

Gulf of Alaska									
Buoy	Model	MSE				SEP (%)			
		Significant Wave Height		Energy Flux		Significant Wave Height		Energy Flux	
		6h	12h	6h	12h	6h	12h	6h	12h
46 001	MTEANN$_Z$	**0.250 2$_{0.006\ 1}$**	**0.491 5$_{0.012\ 3}$**	**458.084 6$_{15.185\ 4}$**	**802.286 7$_{22.446\ 2}$**	**19.786 1$_{0.239\ 8}$**	**27.725 1$_{0.345\ 6}$**	**74.374 8$_{1.234\ 8}$**	**98.395 1$_{1.374\ 5}$**
	MTEANN$_L$	0.2 576$_{0.008\ 3}$	0.5 064$_{0.015\ 6}$	469.9 536$_{27.536\ 4}$	830.9 673$_{49.138\ 4}$	20.0 763$_{0.322\ 8}$	28.1 417$_{0.434\ 0}$	75.3 110$_{2.200\ 7}$	100.1 066$_{2.914\ 6}$
46 066	MTEANN$_Z$	0.2 487$_{0.008\ 7}$	**0.441 4$_{0.009\ 9}$**	**489.100 0$_{22.150\ 1}$**	**768.832 3$_{34.060\ 2}$**	18.1 751$_{0.315\ 1}$	**24.197 5$_{0.270\ 0}$**	**64.409 4$_{1.442\ 2}$**	**80.516 5$_{1.772\ 8}$**
	MTEANN$_L$	**0.246 6$_{0.008\ 7}$**	0.4 614$_{0.021\ 6}$	546.6 133$_{47.036\ 9}$	947.4 676$_{343.866\ 5}$	**18.098 8$_{0.318\ 3}$**	24.7 347$_{0.566\ 2}$	68.0 504$_{2.829\ 3}$	88.6 155$_{11.993\ 7}$
46 085	MTEANN$_Z$	**0.231 4$_{0.005\ 9}$**	**0.471 2$_{0.011\ 4}$**	424.4 362$_{19.422\ 9}$	**722.014 2$_{35.011\ 4}$**	**18.509 7$_{0.236\ 0}$**	**26.407 4$_{0.318\ 6}$**	66.4 036$_{1.497\ 8}$	**86.551 3$_{2.093\ 4}$**
	MTEANN$_L$	0.2 427$_{0.022\ 3}$	0.5 070$_{0.071\ 3}$	**418.032 3$_{20.681\ 0}$**	746.7 580$_{47.401\ 2}$	18.9 394$_{0.822\ 8}$	27.3 440$_{1.702\ 3}$	**65.897 6$_{1.621\ 5}$**	88.0 054$_{2.739\ 6}$

The best result is highlighted in **bold**.

Table 5
Comparison between zonal and local MTEANN models (i.e. $MTEANN_Z$ models and $MTEANN_L$ models, respectively) in terms of the number of connections for the different buoys located in both coastal zones. The results are expressed as their mean and Standard Deviation (SD): $Mean_{SD}$.

South West Coast			
Model	Buoy	*#Conn* Ind.	*#Conn*
$MTEANN_Z$	–	–	$\mathbf{271.25_{9.29}}$
$MTEANN_L$	46 011	$272.45_{9.91}$	$813.53_{20.64}$
	46 047	$271.43_{10.97}$	
	46 069	$269.65_{14.59}$	
Gulf of Alaska			
Model	Buoy	*#Conn* Ind.	*#Conn*
$MTEANN_Z$	–	–	$\mathbf{268.75_{13.27}}$
$MTEANN_L$	46 001	$272.75_{9.44}$	$812.10_{16.74}$
	46 066	$269.58_{12.44}$	
	46 085	$269.78_{10.27}$	

The best result is highlighted in **bold**.

Table 6
Results achieved by the state-of-the-art models in terms of MSE and SEP for the different buoys located in both coastal zones. The results for the $MTEANN_Z$ model are expressed as their mean and Standard Deviation (SD): $Mean_{SD}$.

South West Coast									
Buoy	Model	MSE				SEP (%)			
		Significant Wave Height		Energy Flux		Significant Wave Height		Energy Flux	
		6h	12h	6h	12h	6h	12h	6h	12h
46 011	$MTEANN_Z$	$0.0\ 987_{0.001\ 4}$	$\mathit{0.182\ 2_{0.002\ 7}}$	$\mathbf{96.059\ 4_{1.701\ 9}}$	$\mathbf{158.027\ 0_{4.029\ 3}}$	$15.7\ 674_{0.112\ 3}$	$\mathit{21.410\ 8_{0.156\ 6}}$	$\mathbf{56.255\ 5_{0.497\ 6}}$	$\mathbf{72.079\ 7_{0.915\ 2}}$
	SVR_Z	**0.090 0**	**0.172 0**	137.418 4	196.913 4	**14.921 6**	**20.639 6**	65.767 6	78.776 1
	$LinearReg_Z$	*0.097 9*	0.189 5	124.550 7	*181.789 7*	*15.568 1*	21.665 6	62.612 7	*75.690 5*
	$RidgeReg_Z$	*0.097 9*	0.189 5	124.550 7	*181.789 7*	*15.568 1*	21.665 6	62.612 7	*75.690 5*
	$LassoReg_Z$	*0.097 9*	0.189 5	*124.549 1*	181.791 4	*15.568 1*	21.665 5	*62.612 3*	75.690 9
	$ElasticNet_Z$	*0.097 9*	0.189 5	*124.549 1*	181.791 4	*15.568 1*	21.665 5	*62.612 3*	75.690 9
46 047	$MTEANN_Z$	$\mathit{0.093\ 6_{0.001\ 6}}$	$\mathit{0.178\ 3_{0.003\ 0}}$	$\mathbf{119.809\ 6_{2.720\ 3}}$	$200.6\ 619_{6.356\ 0}$	$\mathbf{14.892\ 0_{0.123\ 3}}$	$\mathit{20.538\ 7_{0.172\ 4}}$	$\mathbf{58.692\ 9_{0.663\ 9}}$	$\mathbf{75.863\ 2_{1.184\ 2}}$
	SVR_Z	**0.089 3**	**0.160 1**	129.168 6	177.958 5	*15.010 5*	**20.107 6**	67.035 7	78.734 8
	$LinearReg_Z$	0.099 4	*0.181 0*	128.565 5	*169.833 1*	15.837 3	21.381 3	66.879 1	76.916 3
	$RidgeReg_Z$	0.099 4	*0.181 0*	128.565 5	*169.833 1*	15.837 3	21.381 3	66.879 1	76.916 3
	$LassoReg_Z$	0.099 4	*0.181 0*	*128.562 7*	**169.830 0**	15.837 2	21.381 2	*66.878 3*	*76.915 6*
	$ElasticNet_Z$	0.099 4	*0.181 0*	*128.562 7*	**169.830 0**	15.837 2	21.381 2	*66.878 3*	*76.915 6*
46 069	$MTEANN_Z$	$\mathbf{0.098\ 8_{0.001\ 8}}$	$\mathbf{0.183\ 7_{0.002\ 8}}$	$\mathbf{147.795\ 6_{5.074\ 9}}$	$\mathbf{237.545\ 5_{4.764\ 3}}$	$\mathit{15.034\ 9_{0.139\ 5}}$	$\mathit{20.488\ 0_{0.155\ 0}}$	$64.0\ 926_{1.091\ 8}$	$81.1\ 812_{0.810\ 9}$
	SVR_Z	*0.102 4*	*0.193 7*	182.868 8	276.010 6	**14.349 2**	**19.734 5**	57.671 6	70.824 2
	$LinearReg_Z$	0.116 6	0.224 5	*155.321 0*	*238.228 5*	15.316 8	21.246 5	**53.150 5**	**65.798 5**
	$RidgeReg_Z$	0.116 6	0.224 5	*155.321 0*	*238.228 5*	15.316 8	21.246 5	**53.150 5**	**65.798 5**
	$LassoReg_Z$	0.116 6	0.224 5	155.322 9	238.230 2	15.316 9	21.246 6	*53.150 8*	*65.798 7*
	$ElasticNet_Z$	0.116 6	0.224 5	155.322 9	238.230 2	15.316 9	21.246 6	*53.150 8*	*65.798 7*

Gulf of Alaska									
Buoy	Model	MSE				SEP (%)			
		Significant Wave Height		Energy Flux		Significant Wave Height		Energy Flux	
		6h	12h	6h	12h	6h	12h	6h	12h
46 001	$MTEANN_Z$	$\mathbf{0.250\ 2_{0.006\ 1}}$	$\mathbf{0.491\ 5_{0.012\ 3}}$	$\mathbf{458.084\ 6_{15.185\ 4}}$	$\mathbf{802.286\ 7_{22.446\ 2}}$	$\mathbf{19.786\ 1_{0.239\ 8}}$	$\mathbf{27.725\ 1_{0.345\ 6}}$	$\mathbf{74.374\ 8_{1.234\ 8}}$	$\mathbf{98.395\ 1_{1.374\ 5}}$
	SVR_Z	*0.262 3*	*0.513 5*	739.191 7	1007.570 3	*20.258 3*	*28.340 0*	94.490 9	110.277 7
	$LinearReg_Z$	0.338 4	0.659 7	665.149 4	994.411 7	23.011 3	32.121 7	89.633 7	109.555 3
	$RidgeReg_Z$	0.338 4	0.659 5	665.076 5	*994.301 5*	23.010 2	32.118 6	89.628 7	*109.549 2*
	$LassoReg_Z$	0.338 6	0.660 7	*664.772 6*	995.070 8	23.019 1	32.147 9	*89.608 3*	109.591 6
	$ElasticNet_Z$	0.338 6	0.660 7	*664.772 6*	995.070 8	23.019 1	32.147 9	*89.608 3*	109.591 6
46 066	$MTEANN_Z$	$\mathit{0.248\ 7_{0.008\ 7}}$	$\mathit{0.441\ 4_{0.009\ 9}}$	$\mathbf{489.100\ 0_{22.150\ 1}}$	$\mathbf{768.832\ 3_{34.060\ 2}}$	$\mathit{18.175\ 1_{0.315\ 1}}$	$\mathit{24.197\ 5_{0.270\ 0}}$	$\mathbf{64.409\ 4_{1.442\ 2}}$	$\mathbf{80.516\ 5_{1.772\ 8}}$
	SVR_Z	**0.243 9**	**0.436 4**	559.376 8	791.492 1	**18.003 2**	**24.062 2**	68.898 3	81.713 7
	$LinearReg_Z$	0.301 6	0.538 4	533.821 4	774.604 0	20.019 3	26.725 8	67.306 1	80.837 3
	$RidgeReg_Z$	0.301 4	0.538 3	533.588 3	774.417 5	20.014 3	26.721 7	67.291 4	80.827 5
	$LassoReg_Z$	0.302 7	0.543 8	*533.088 3*	*774.296 4*	20.056 3	26.858 8	*67.259 8*	*80.821 2*
	$ElasticNet_Z$	0.302 7	0.543 8	*533.088 3*	*774.296 4*	20.056 3	26.858 8	*67.259 8*	*80.821 2*
46 085	$MTEANN_Z$	$\mathbf{0.231\ 4_{0.005\ 9}}$	$\mathbf{0.471\ 2_{0.011\ 4}}$	$\mathbf{424.436\ 2_{19.422\ 9}}$	$\mathbf{722.014\ 2_{35.011\ 4}}$	$\mathbf{18.509\ 7_{0.236\ 0}}$	$\mathbf{26.407\ 4_{0.318\ 6}}$	$\mathbf{66.403\ 6_{1.497\ 8}}$	$\mathbf{86.551\ 3_{2.093\ 4}}$
	SVR_Z	*0.245 5*	*0.495 9*	662.319 7	941.049 0	*19.065 2*	*27.092 0*	82.971 1	98.839 5
	$LinearReg_Z$	0.317 9	0.623 7	620.281 7	915.312 7	21.695 7	30.384 3	80.294 8	97.478 6
	$RidgeReg_Z$	0.317 8	0.623 7	620.091 0	*915.231 0*	21.693 5	30.383 7	80.282 5	*97.474 2*
	$LassoReg_Z$	0.320 2	0.630 5	*619.218 6*	915.870 2	21.774 7	30.549 7	*80.226 0*	97.508 3
	$ElasticNet_Z$	0.320 2	0.630 5	*619.218 6*	915.870 2	21.774 7	30.549 7	*80.226 0*	97.508 3

The best result is highlighted in **bold**; the second one best result is shown in *italics*.

Table 7
Comparison between the $MTEANN_Z$ model and the state-of-the-art models in terms of the number of connections for the different buoys located in both coastal zones. The results for the $MTEANN_Z$ model are expressed as their mean and Standard Deviation (SD): $Mean_{SD}$.

	South West Coast					
	$MTEANN_Z$	SVR_Z	$LinearReg_Z$	$RidgeReg_Z$	$LassoReg_Z$	$ElasticNet_Z$
#Conn	$271.25_{9.29}$	442 228.00	*40.00*	*40.00*	**37.00**	**37.00**
	Gulf of Alaska					
	$MTEANN_Z$	SVR_Z	$LinearReg_Z$	$RidgeReg_Z$	$LassoReg_Z$	$ElasticNet_Z$
#Conn	$268.75_{13.27}$	463 378.00	*40.00*	*40.00*	**33.00**	**33.00**

The best result is highlighted in **bold**; the second one best result is shown in *italics*.

Table 8
Ranks obtained for the comparison against the state-of-the-art techniques for both coastal zones considered.

	$MTEANN_Z$	SVR_Z	$LinearReg_Z$	$RidgeReg_Z$	$LassoReg_Z$	$ElasticNet_Z$
Ranks MSE	**1.625**	3.708	4.125	*3.375*	3.583	3.583
Ranks SEP	**1.875**	3.625	4.083	*3.333*	3.542	3.542

The best result is highlighted in **bold**; the second one best result is shown in *italics*.

competitive approach for the problem tackled. As previously, the results are shown in terms of both performance measures, MSE and SEP for each output individually (Table 6), and in terms of complexity (*#Conn*, Table 7) for both coastal zones (South West Coast and Gulf of Alaska).

In general, it can be seen in Table 6 that, for most of the buoys, $MTEANN_Z$ methodology is able to achieve the better results than the rest of the approaches. From a quantitative point of view, the proposed methodology obtains the best results in 32 comparisons and the second best in other 11, from a total of 48 comparisons. At a glance, it could be said that the $MTEANN_Z$ model achieves competitive results for both tasks. Regarding the complexity of the different models, Table 7 shows the number of connections (*#Conn*) for each of these techniques, demonstrating that simpler models such as $LinearReg_Z$, $RidgeReg_Z$, $LassoReg_Z$ or $ElasticNet_Z$ have no competitors in terms of complexity (*#Conn*).

Furthermore, in order to establish a robust comparison between our proposal ($MTEANN_Z$) and the main state-of-the-art techniques, Table 8 shows the ranks achieved by the different approaches for each performance measure. This last comparison is done to provide the reader with a more specific summary of the results reported in Table 6. The procedure followed starts by computing the average of the ranks obtained for each of the four outputs (1 for the method involving the lowest error, while 6 for the one resulting in the highest one), individually. Then, they are averaged for each buoy, giving, in this way, a more general point of view of the methodology proposed in this paper. As can be seen from this Table, the $MTEANN_Z$ model is the one achieving the best results with ranks of 1.625 in terms of MSE and 1.875 in case of SEP. On the other hand, the second best method is the $RidgeReg_Z$, with ranks 3.375 and 3.333 considering MSE and SEP, respectively. It is worthy of mention that there is a huge gap between the $MTEANN_Z$ model and the rest of the techniques, indicating, in this sense, that this algorithm achieves an excellent performance.

These results demonstrate that combining the zonal strategy with the multi-task learning applied to EANNs is an excellent

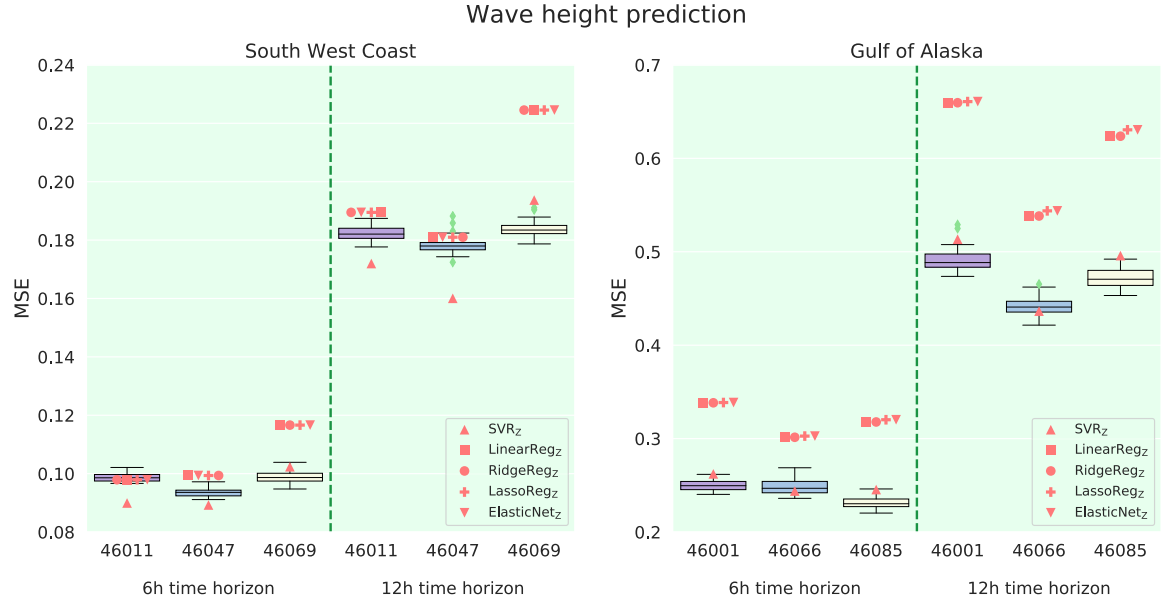

Fig. 6. Box-plot obtained from the 40 runs of $MTEANN_Z$ model for the two zones considered regarding the significant wave height prediction made at 6h and 12h time prediction horizons and MSE performance measure. The results of the state-of-the-art techniques are also represented according to their deterministic value.

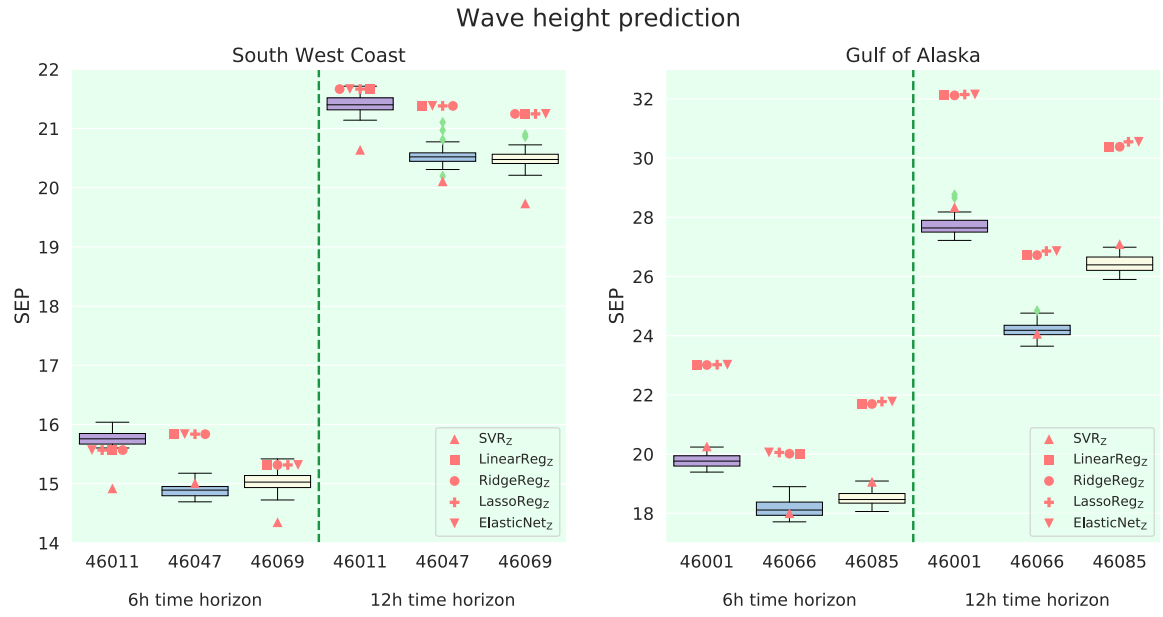

Fig. 7. Box-plot obtained from the 40 runs of MTEANN$_Z$ model for the two zones considered regarding the significant wave height prediction made at 6h and 12h time prediction horizons and SEP performance measure. The results of the state-of-the-art techniques are also represented according to their deterministic value.

model for related tasks (in this case, significant wave height and energy flux prediction). Not only does it improve the performance achieved by local models individually-trained for each buoy, but also, it is able to obtain better results than the main state-of-the-art techniques in the literature, also taking into account the zonal strategy. One of the reasons is that the multi-task paradigm benefits from already learned tasks to reduce the error in other related tasks, such is the case of significant wave height and energy flux, being more efficient for the problem tackled.

Apart from computing the ranks, in order to compare in a graphical way the results showed in Table 6 and to ease the readability of this paper, Figs. 6–9 show the box-plots of the MTEANN$_Z$ model (i.e. the distribution of the 40 runs). In addition, the results achieved by the state-of-the-art techniques are also shown in these figures. Specifically, Figs. 6 and 7 show the box-plots for the significant wave height prediction at 6h and 12h time prediction horizons in both coastal zones for the MSE and SEP, respectively. While Figs. 8 and 9 show, in the same way, the flux of energy prediction also regarding the MSE and SEP, respectively.

From these figures, we can appreciate that the MTEANN$_Z$ models are robust and stable for most buoys (i.e. the number of runs that could be considered as outliers is small), presenting a low standard deviation. Moreover, the MTEANN$_Z$ model shows higher predictive accuracy as compared to the other models in this study.

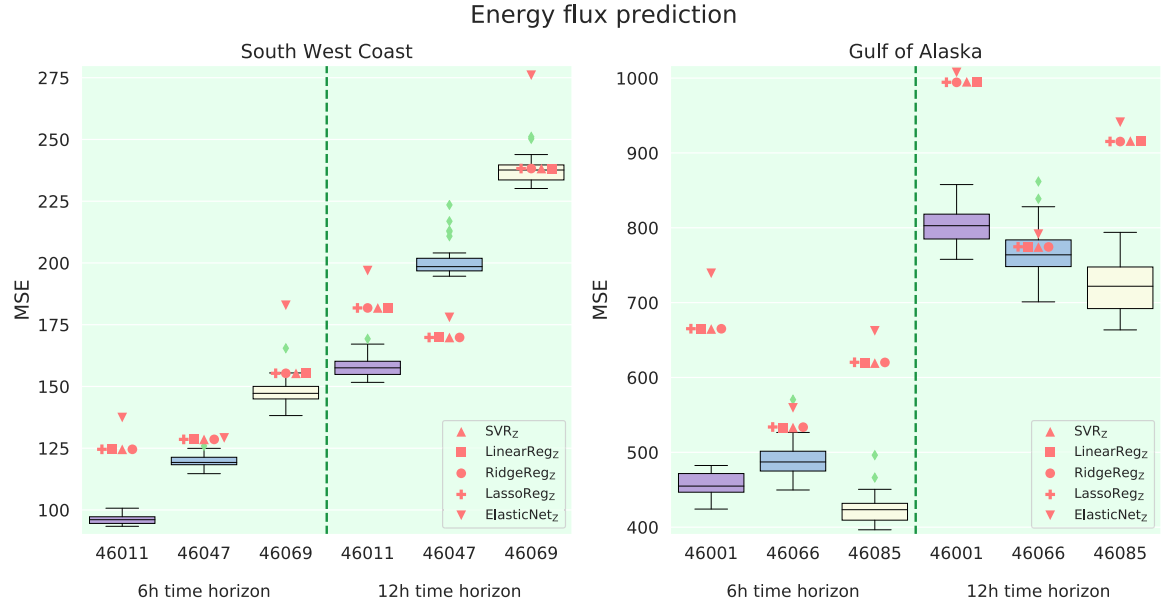

Fig. 8. Box-plot obtained from the 40 runs of MTEANN$_Z$ model for the two zones considered regarding the energy flux prediction made at 6h and 12h time prediction horizons and MSE performance measure. The results of the state-of-the-art techniques are also represented according to their deterministic value.

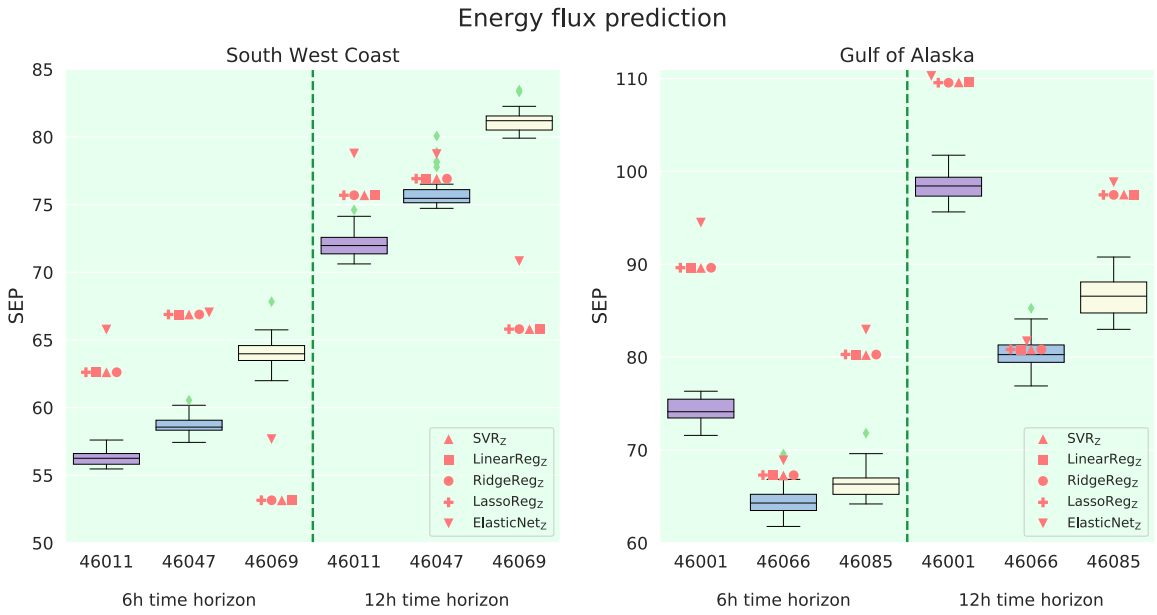

Fig. 9. Box-plot obtained from the 40 runs of MTEANN$_Z$ model for the two zones considered regarding the energy flux prediction made at 6h and 12h time prediction horizons and SEP performance measure. The results of the state-of-the-art techniques are also represented according to their deterministic value.

Regarding the computational cost of the proposed zonal methodology (MTEANN$_Z$ model), the Mean and Standard Deviation (*Mean*$_{SD}$ of the 40 runs) corresponding to the training runtime is $213.36_{28.53}$ h for the South West Coast zone, and $215.79_{36.28}$ h for the Gulf of Alaska zone. It is worthy of mention that once the model has been optimised (training phase) the runtime of the test phase is negligible.

5. Conclusions

In this paper, we have proposed a novel methodology able to predict the significant wave height and the flux of energy simultaneously. Moreover, apart from developing models able to accurately predict both tasks, in this paper, we have focused on conceiving a novel strategy (known as zonal strategy) based on the development of a unique model able to accurately estimate predictions for all the buoys located in the same zone. Specifically, we have considered two main zones given its interest in the literature: the South West Coast (buoys 46 011, 46 047 and 46 069) and the Gulf of Alaska (buoys 46 001, 46 066 and 46 085). Regarding the input data used, reanalysis data, which benefits from the absence of missing values, it has been combined with past values of the significant wave height and the average wave period, which improve the performance of the models. Moreover, the two target variables have been taken at two time prediction horizons (6h and 12h), representing short-term prediction horizons. In this way, we have proposed the mixture of the zonal methodology with Multi-Task Evolutionary Artificial Neural Network (MTEANN$_Z$) models, focusing on a MTEANN$_Z$ model combining sigmoid units in the hidden layer with linear units in the output layer. Two sort of comparisons have been carried out in order to demonstrated the usefulness of the proposal. First of all, MTEANN$_Z$ model has been compared against the independent training of MTEANN$_L$ models, with one model for each buoy. The results of this first comparison demonstrated that the zonal strategy achieved better results in terms of Mean Square Error (MSE), Standard Error of Prediction (SEP) and complexity (*#Conn*), and, therefore, the use of the zonal strategy was justified. On the other hand, the second comparison was carried out against some of the most popular approaches in the state-of-the-art, such as Support Vector Regressors (SVR), Lasso regression or ElasticNet, among others. In this second comparison, all approaches followed the zonal strategy, but the MTEANN$_Z$ model also achieved the best performance in terms of MSE and SEP, while not in terms of complexity (*#Conn*) where linear models have no competitors. Hence, it has been demonstrated that the proposed approach combining MTEANN models and the zonal strategy (MTEANN$_Z$) has an enormous potential for this kind of applications achieving a high level of accuracy. As future research, it will be interesting to broaden the study including more locations and developing a novel methodology combining zonal models in such a way that the training stage could be even simpler without a big loss in the accuracy. Furthermore, it could be of interest to analyse the applicability of the zonal models to predict within the area delimited by the buoys of the zone.

CRediT authorship contribution statement

A.M. Gómez-Orellana: Methodology, Software, Validation, Investigation, Data curation, Writing – original draft. **D. Guijo-Rubio:** Methodology, Validation, Formal analysis, Investigation, Writing – original draft, Visualization. **P.A. Gutiérrez:** Conceptualization, Software, Formal analysis, Writing – review & editing. **C. Hervás-Martínez:** Conceptualization, Resources, Supervision, Project administration, Funding acquisition.

Declaration of competing interest

The authors declare that they have no known competing financial interests or personal relationships that could have appeared to influence the work reported in this paper.

Acknowledgements

This work has been partially subsidised by “Ministerio de Economía y Competitividad del Gobierno de España y Fondos FEDER” (grant reference: TIN2017-85 887-C2-1-P), by “Agencia

Española de Investigación (España)" (grant reference: PID2020-115454 GB-C22/AEI/10.130 39/501 100 011 033), by "Consejería de Salud y Familia (Junta de Andalucía)" (grant reference: PS-2020-780), and by "Consejería de Transformación Económica, Industria, Conocimiento y Universidades (Junta de Andalucía) y Programa Operativo FEDER 2014–2020" (grant references: UCO-1261 651 and PY20_00074). The open access charge was fully supported by the Universidad de Córdoba/CBUA.

References

[1] R. Hashim, C. Roy, S. Motamedi, S. Shamshirband, D. Petković, Selection of climatic parameters affecting wave height prediction using an enhanced Takagi-Sugeno-based fuzzy methodology, Renew. Sustain. Energy Rev. 60 (2016) 246–257, https://doi.org/10.1016/j.rser.2016.01.098.

[2] L. Cornejo-Bueno, E.C. Garrido-Merchán, D. Hernández-Lobato, S. Salcedo-Sanz, Bayesian optimization of a hybrid system for robust ocean wave features prediction, Neurocomputing 275 (2018) 818–828, https://doi.org/10.1016/j.neucom.2017.09.025.

[3] R. Asariotis, H. Benamara, Maritime Transport and the Climate Change Challenge, Routledge, 2012, https://doi.org/10.4324/9780203134467.

[4] R.C. Geronimo, E.C. Franklin, R.E. Brainard, C.D. Elvidge, M.D. Santos, R. Venegas, C. Mora, Mapping fishing activities and suitable fishing grounds using nighttime satellite images and maximum entropy modelling, Rem. Sens. 10 (10) (2018) 1604, https://doi.org/10.3390/rs10101604.

[5] S. Yusop, M. Mustapha, Influence of oceanographic parameters on the seasonal potential fishing grounds of Rastrelliger kanagurta using maximum entropy models and remotely sensed data, Sains Malays. 48 (2) (2019) 259–269.

[6] T.B. Johannessen, Ø. Lande, Ø. Hagen, On the distribution of wave impact loads on offshore structures, in: International Conference on Offshore Mechanics and Arctic Engineering, vol. 57656, American Society of Mechanical Engineers, 2017, https://doi.org/10.1115/omae2017-62057. V03AT02A029.

[7] R. Carballo, N. Arean, M. Álvarez, I. López, A. Castro, M. López, G. Iglesias, Wave farm planning through high-resolution resource and performance characterization, Renew. Energy 135 (2019) 1097–1107, https://doi.org/10.1016/j.renene.2018.12.081.

[8] M.A. El-Reedy, Offshore Structures: Design, Construction and Maintenance, Gulf Professional Publishing, 2019, https://doi.org/10.1016/C2010-0-65924-4.

[9] M. Esteban, D. Leary, Current developments and future prospects of offshore wind and ocean energy, Appl. Energy 90 (1) (2012) 128–136, https://doi.org/10.1016/j.apenergy.2011.06.011, energy Solutions for a Sustainable World, Special Issue of International Conference of Applied Energy, ICA2010, April 21-23, 2010, Singapore.

[10] C. Kalogeri, G. Galanis, C. Spyrou, D. Diamantis, F. Baladima, M. Koukoula, G. Kallos, Assessing the European offshore wind and wave energy resource for combined exploitation, Renew. Energy 101 (2017) 244–264, https://doi.org/10.1016/j.renene.2016.08.010.

[11] L. Cuadra, S. Salcedo-Sanz, J. Nieto-Borge, E. Alexandre, G. Rodríguez, Computational intelligence in wave energy: comprehensive review and case study, Renew. Sustain. Energy Rev. 58 (2016) 1223–1246, https://doi.org/10.1016/j.rser.2015.12.253.

[12] J. Wolf, D. K. Woolf, Waves and climate change in the north-east Atlantic, Geophys. Res. Lett. 33 (6). doi:10.1029/2005gl025113.

[13] D. Callaghan, P. Nielsen, A. Short, R. Ranasinghe, Statistical simulation of wave climate and extreme beach erosion, Coast Eng. 55 (5) (2008) 375–390, https://doi.org/10.1016/j.coastaleng.2007.12.003.

[14] P. Malik, S. Singh, B. Arora, An effective weather forecasting using neural network, Int. J. Emerg. Eng.Res.Technol. 2 (2) (2014) 209–212, https://doi.org/10.7763/ijesd.2010.v1.63.

[15] S. Samayam, V. Laface, S.A. Sannasiraj, F. Arena, S. Vallam, P.V. Gavrilovich, Assessment of reliability of extreme wave height prediction models, Nat. Hazards Earth Syst. Sci. 17 (3) (2017) 409, https://doi.org/10.5194/nhess-17-409-2017.

[16] D. Demetriou, C. Michailides, G. Papanastasiou, T. Onoufriou, Coastal zone significant wave height prediction by supervised machine learning classification algorithms, Ocean Eng. 221 (2021) 108592, https://doi.org/10.1016/j.oceaneng.2021.108592.

[17] F. Taveira-Pinto, P. Rosa-Santos, T. Fazeres-Ferradosa, Marine renewable energy, Renew. Energy 150 (2020) 1160–1164, https://doi.org/10.1016/j.renene.2019.10.014.

[18] Z. Defne, K.A. Haas, H.M. Fritz, Wave power potential along the Atlantic coast of the southeastern USA, Renew. Energy 34 (10) (2009) 2197–2205, https://doi.org/10.1016/j.renene.2009.02.019.

[19] P.A. Bonar, I.G. Bryden, A.G. Borthwick, Social and ecological impacts of marine energy development, Renew. Sustain. Energy Rev. 47 (2015) 486–495, https://doi.org/10.1016/j.rser.2015.03.068.

[20] J.V. Hernández-Fontes, M.L. Martínez, A. Wojtarowski, J.L. González-Mendoza, R. Landgrave, R. Silva, Is ocean energy an alternative in developing regions? A case study in Michoacan, Mexico, J. Clean. Prod. (2020) 121984doi, https://doi.org/10.1016/j.jclepro.2020.121984.

[21] R. Alamian, R. Shafaghat, S.J. Miri, N. Yazdanshenas, M. Shakeri, Evaluation of technologies for harvesting wave energy in Caspian Sea, Renew. Sustain. Energy Rev. 32 (2014) 468–476, https://doi.org/10.1016/j.rser.2014.01.036.

[22] J. Henriques, M. Lopes, R. Gomes, L. Gato, A. Falcão, On the annual wave energy absorption by two-body heaving WECs with latching control, Renew. Energy 45 (2012) 31–40, https://doi.org/10.1016/j.renene.2012.01.102.

[23] S.A. Hughes, Physical Models and Laboratory Techniques in Coastal Engineering, vol. 7, World Scientific, 1993, https://doi.org/10.1142/2154.

[24] G. Ibarra-Berastegi, J. Saénz, G. Esnaola, A. Ezcurra, A. Ulazia, Short-term forecasting of the wave energy flux: analogues, random forests, and physics-based models, Ocean Eng. 104 (2015) 530–539, https://doi.org/10.1016/j.oceaneng.2015.05.038.

[25] E. Vanem, Joint statistical models for significant wave height and wave period in a changing climate, Mar. Struct. 49 (2016) 180–205, https://doi.org/10.1016/j.marstruc.2016.06.001.

[26] Y. Lin, S. Dong, S. Tao, Modelling long-term joint distribution of significant wave height and mean zero-crossing wave period using a copula mixture, Ocean Eng. 197 (2020) 106856, https://doi.org/10.1016/j.oceaneng.2019.106856.

[27] X.G. Larsén, C. Kalogeri, G. Galanis, G. Kallos, A statistical methodology for the estimation of extreme wave conditions for offshore renewable applications, Renew. Energy 80 (2015) 205–218, https://doi.org/10.1016/j.renene.2015.01.069.

[28] C.M. Bishop, Pattern Recognition and Machine Learning, Springer, 2006.

[29] J. Fernández, S. Salcedo-Sanz, P. Gutiérrez, E. Alexandre, C. Hervás-Martínez, Significant wave height and energy flux range forecast with machine learning classifiers, Eng. Appl. Artif. Intell. 43 (2015) 44–53, https://doi.org/10.1016/j.engappai.2015.03.012.

[30] M. Deo, A. Jha, A. Chaphekar, K. Ravikant, Neural networks for wave forecasting, Ocean Eng. 28 (7) (2001) 889–898, https://doi.org/10.1016/S0029-8018(00)00027-5.

[31] O. Makarynskyy, A. Pires-Silva, D. Makarynska, C. Ventura-Soares, Artificial neural networks in wave predictions at the west coast of Portugal, Comput. Geosci. 31 (4) (2005) 415–424, https://doi.org/10.1016/j.cageo.2004.10.005.

[32] A. Castro, R. Carballo, G. Iglesias, J. Rabuñal, Performance of artificial neural networks in nearshore wave power prediction, Appl. Soft Comput. 23 (2014) 194–201, https://doi.org/10.1016/j.asoc.2014.06.031.

[33] P. Abhigna, S. Jerritta, R. Srinivasan, V. Rajendran, Analysis of feed forward and recurrent neural networks in predicting the significant wave height at the moored buoys in Bay of Bengal, in: 2017 International Conference on Communication and Signal Processing (ICCSP), IEEE, 2017, pp. 1856–1860, https://doi.org/10.1109/iccsp.2017.8286717.

[34] T. Sadeghifar, M. Nouri Motlagh, M. Torabi Azad, M. Mohammad Mahdizadeh, Coastal wave height prediction using recurrent neural networks (RNNs) in the South Caspian Sea, Mar. Geodes. 40 (6) (2017) 454–465, https://doi.org/10.1080/01490419.2017.1359220.

[35] J. Berbić, E. Ocvirk, D. Carević, G. Lončar, Application of neural networks and support vector machine for significant wave height prediction, Oceanologia 59 (3) (2017) 331–349, https://doi.org/10.1016/j.oceano.2017.03.007.

[36] N.K. Kumar, R. Savitha, A.A. Mamun, Ocean wave height prediction using ensemble of Extreme Learning Machine, Neurocomputing 277 (2018) 12–20, https://doi.org/10.1016/j.neucom.2017.03.092.

[37] H. Choi, M. Park, G. Son, J. Jeong, J. Park, K. Mo, P. Kang, Real-time significant wave height estimation from raw ocean images based on 2D and 3D deep neural networks, Ocean Eng. 201 (2020) 107129, https://doi.org/10.1016/j.oceaneng.2020.107129.

[38] S. Yang, Z. Deng, X. Li, C. Zheng, L. Xi, J. Zhuang, Z. Zhang, Z. Zhang, A novel hybrid model based on STL decomposition and one-dimensional convolutional neural networks with positional encoding for significant wave height forecast, Renew. Energy 173 (2021) 531–543, https://doi.org/10.1016/j.renene.2021.04.010.

[39] S. Fan, N. Xiao, S. Dong, A novel model to predict significant wave height based on long short-term memory network, Ocean Eng. 205 (2020) 107298, https://doi.org/10.1016/j.oceaneng.2020.107298.

[40] A.S. Sánchez, D.A. Rodrigues, R.M. Fontes, M.F. Martins, R.d.A. Kalid, E.A. Torres, Wave resource characterization through in-situ measurement followed by artificial neural networks' modeling, Renew. Energy 115 (2018) 1055–1066, https://doi.org/10.1016/j.renene.2017.09.032.

[41] P. Bento, J. Pombo, R. Mendes, M. Calado, S. Mariano, Ocean wave energy forecasting using optimised deep learning neural networks, Ocean Eng. 219 (2021) 108372, https://doi.org/10.1016/j.oceaneng.2020.108372.

[42] D. Guijo-Rubio, A.M. Gómez-Orellana, P.A. Gutiérrez, C. Hervás-Martínez, Short-and long-term energy flux prediction using multi-task evolutionary artificial neural networks, Ocean Eng. 216 (2020) 108089, https://doi.org/10.1016/j.oceaneng.2020.108089.

[43] L. Cornejo-Bueno, J. Nieto-Borge, P. García-Díaz, G. Rodríguez, S. Salcedo-Sanz, Significant wave height and energy flux prediction for marine energy applications: a grouping genetic algorithm – extreme Learning Machine approach, Renew. Energy 97 (2016) 380–389, https://doi.org/10.1016/j.renene.2016.05.094.

[44] L. Cornejo-Bueno, P. Rodríguez-Mier, M. Mucientes, J. Nieto-Borge, S. Salcedo-Sanz, Significant wave height and energy flux estimation with a Genetic Fuzzy System for regression, Ocean Eng. 160 (2018) 33–44, https://doi.org/10.1016/j.oceaneng.2018.04.063.

[45] R. Caruana, Multitask Learning, Machine Learning 28 (1) (1997) 41–75,

https://doi.org/10.1023/A:1007379606734.
[46] A. Maurer, M. Pontil, B. Romera-Paredes, The benefit of multitask representation learning, J. Mach. Learn. Res. 17 (1) (2016) 2853–2884, https://doi.org/10.5555/2946645.3007034.
[47] M. Dorado-Moreno, N. Navarin, P. Gutiérrez, L. Prieto, A. Sperduti, S. Salcedo-Sanz, C. Hervás-Martínez, Multi-task learning for the prediction of wind power ramp events with deep neural networks, Neural Network. 123 (2020) 401–411, https://doi.org/10.1016/j.neunet.2019.12.017.
[48] National data buoy center, national oceanic and atmospheric administration of the USA (NOAA). http://www.ndbc.noaa.gov/, 2020. (Accessed 1 June 2020).
[49] E. Kalnay, M. Kanamitsu, R. Kistler, W. Collins, D. Deaven, L. Gandin, M. Iredell, S. Saha, G. White, J. Woollen, Y. Zhu, A. Leetmaa, R. Reynolds, M. Chelliah, W. Ebisuzaki, W. Higgins, J. Janowiak, K.C. Mo, C. Ropelewski, J. Wang, R. Jenne, D. Joseph, The NCEP/NCAR 40-year reanalysis Project, Bull. Am. Meteorol. Soc. 77 (3) (1996) 437–471, https://doi.org/10.1175/1520-0477(1996)077<0437:TNYRP>2.0.CO;2.
[50] R. Kistler, W. Collins, S. Saha, G. White, J. Woollen, E. Kalnay, M. Chelliah, W. Ebisuzaki, M. Kanamitsu, V. Kousky, H. van den Dool, R. Jenne, M. Fiorino, The NCEP–NCAR 50–year reanalysis: monthly means CD–ROM and documentation, Bull. Am. Meteorol. Soc. 82 (2) (2001) 247–267, https://doi.org/10.1175/1520-0477(2001)082<0247:TNNYRM>2.3.CO;2.
[51] NDBC - station 46011, NDBC - station 46011 recent data. https://www.ndbc.noaa.gov/station_page.php?station=46011, 2020. (Accessed 1 June 2020).
[52] NDBC - station 46047, NDBC - station 46047 recent data. https://www.ndbc.noaa.gov/station_page.php?station=46047, 2020. (Accessed 1 June 2020).
[53] NDBC - station 46069, NDBC - station 46069 recent data. https://www.ndbc.noaa.gov/station_page.php?station=46069, 2020. (Accessed 1 June 2020).
[54] NDBC - station 46001, NDBC - station 46001 recent data. https://www.ndbc.noaa.gov/station_page.php?station=46001, 2020. (Accessed 1 June 2020).
[55] NDBC - station 46066, NDBC - station 46066 recent data. https://www.ndbc.noaa.gov/station_page.php?station=46066, 2020. (Accessed 1 June 2020).
[56] NDBC - station 46085, NDBC - station 46085 recent data. https://www.ndbc.noaa.gov/station_page.php?station=46085, 2020. (Accessed 1 June 2020).
[57] A.M. Gómez-Orellana, J.C. Fernández, M. Dorado-Moreno, P.A. Gutiérrez, C. Hervás-Martínez, Building suitable datasets for soft computing and machine learning techniques from meteorological data integration: a case study for predicting significant wave height and energy flux, Energies 14 (2) (2021) 468, https://doi.org/10.3390/en14020468.
[58] C.M. Bishop, et al., Neural Networks for Pattern Recognition, Oxford University Press, 1995.
[59] R.P. Lippmann, Pattern classification using neural networks, IEEE Commun. Mag. 27 (11) (1989) 47–50, https://doi.org/10.1109/35.41401.
[60] D. Guijo-Rubio, A.M. Durán-Rosal, P.A. Gutiérrez, A.M. Gómez-Orellana, C. Casanova-Mateo, J. Sanz-Justo, S. Salcedo-Sanz, C. Hervás-Martínez, Evolutionary artificial neural networks for accurate solar radiation prediction, Energy 210 (2020) 1–11, https://doi.org/10.1016/j.energy.2020.118374.
[61] P.J. Angeline, G.M. Saunders, J.B. Pollack, An evolutionary algorithm that constructs recurrent neural networks, Trans. Neur. Netw. 5 (1) (1994) 54–65, https://doi.org/10.1109/72.265960.
[62] L. Prechelt, et al., Proben1: A set of neural network benchmark problems and benchmarking rules, Tech. rep., Fakultät für Informatik, Universität Karlsruhe, 1994.
[63] A. Martínez-Estudillo, F. Martínez-Estudillo, C. Hervás-Martínez, N. García-Pedrajas, Evolutionary product unit based neural networks for regression, Neural Network. 19 (4) (2006) 477–486, https://doi.org/10.1016/j.neunet.2005.11.001.
[64] C. Hervás, P.A. Gutierrez, M. Silva, J.M. Serrano, Combining classification and regression approaches for the quantification of highly overlapping capillary electrophoresis peaks by using evolutionary sigmoidal and product unit neural networks, J. Chemometr. 21 (12) (2007) 567–577, https://doi.org/10.1002/cem.1082.
[65] J.C. Fernandez Caballero, F.J. Martinez, C. Hervas, P.A. Gutierrez, Sensitivity versus accuracy in multiclass problems using memetic pareto evolutionary neural networks, IEEE Trans. Neural Network. 21 (5) (2010) 750–770, https://doi.org/10.1109/TNN.2010.2041468.
[66] V. Vapnik, The Nature of Statistical Learning Theory, Springer science & business media, 2013, https://doi.org/10.1007/978-1-4757-2440-0.
[67] J. Friedman, T. Hastie, R. Tibshirani, Regularization paths for generalized linear models via coordinate descent, Journal of Statistical Software, Articles 33 (1) (2010) 1–22.
[68] H. Zou, T. Hastie, Regularization and variable selection via the elastic net, J. Roy. Stat. Soc. B 67 (2) (2005) 301–320, https://doi.org/10.1111/j.1467-9868.2005.00503.x.